The Homerian (Silurian) stratigraphy of the May Hill and Gorsley inliers of England, UK: integration of carbon isotope data, sedimentology, and sequence stratigraphy

David C. Ray, James R. Wheeley, Georgia Hazeldine, Adrian Burrows & Stephen Kershaw

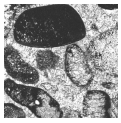

The globally-recognised Homerian (Silurian) carbon isotope excursion (CIE) occurs in the Much Wenlock Limestone Formation and Gorsley Limestone of the May Hill and Gorsley inliers of the southern part of the Midland Platform (eastern Avalonia), England. This CIE is associated with eustatic sea-level fluctuations and time-specific facies, and is documented in limestone facies formed in a tropical shallow marine setting, that crop out at the key localities of Hobbs Quarry, Hobbs Lane, and Linton Quarry. Carbon isotope trends and values from these localities identify the falling limbs of the first and second peaks of the Homerian CIE at Hobbs Quarry and Hobbs Lane, respectively, and the low between these peaks at Linton Quarry. The identification and correlation of these parts of the Homerian CIE, alongside the correlation of lithofacies, bentonites and sea-level changes, indicate that at May Hill, the Much Wenlock Limestone Formation began near the top of Silurian stage slice Ho1 and ended near the top of Ho3 (*i.e.* middle to end Homerian), as is the case for the inner part of the Midland Platform to the north of the study area. Lithofacies of the Gorsley Limestone (Gorsley Inlier), alongside carbon isotope values, correlate to the middle of the Much Wenlock Limestone Formation, as developed at May Hill and across the inner part of the Midland Platform. This indicates that the unconformity at the top of the Gorsley Limestone omits the latest Homerian limestones and second peak of the Homerian CIE, as well as the overlying Gorstian. Furthermore, the uplift, subaerial exposure, and weathering of pyrite-rich sediments in the Gorsley area, to form the Gorsley High, may have supplied iron into the surrounding marine environment, and resulted in the localised development of the latest Homerian ferruginous crinoidal grainstones of the neighbouring May Hill Inlier and Ledbury Hills. These results demonstrate that the CIE and associated strata in the study sites are consistent with regional trends, and therefore add to the global database of these mid-Silurian stratigraphic changes. • Key words: Silurian, Wenlock, carbon isotope, stratigraphy, May Hill, Midland Platform, Avalonia.

Ray, D.C., Wheeley, J.R., Hazeldine, G., Burrows, A. & Kershaw, S. 2025. The Homerian (Silurian) stratigraphy of the May Hill and Gorsley inliers of England, UK: integration of carbon isotope data, sedimentology, and sequence stratigraphy. *Bulletin of Geosciences 100*(*4*), 489–504 (6 figures, 1 table). Czech Geological Survey, Prague. ISSN 1214-1119. Manuscript received February 25, 2025; accepted in revised form July 2, 2025; published online July 20, 2025; issued December 31, 2025.

David C. Ray (corresponding author), James R. Wheeley & Georgia Hazeldine, School of Geography, Earth and Environmental Sciences (GEES), University of Birmingham, UK; daveray01@yahoo.com • Adrian Burrows, Hobbs Nature Reserve Trust, Longhope, Gloucestershire, UK • Stephen Kershaw, Department of Earth Sciences, Brunel University, UK; Science Group, Natural History Museum, London, UK

In central England, the inliers of May Hill and Gorsley form part of a discontinuous belt of Silurian strata between the outcrops of the Ledbury, Malvern, Suckley and Abberley hills to the north and the Tortworth Inlier to the south (Fig. 1). During Homerian times (late Wenlock Series) the May Hill and Gorsley study area and the wider Midland Platform were part of a gently subsiding shallow marine shelf, which occupied the Welsh Borders and much of central England (Bassett *et al.* 1992). From a global perspective the Midland Platform formed part of the eastern Avalonia microcontinent and was situated between 30° and 13° S of the equator (Torsvik *et al.* 1993, Golonka *et al.* 2023). This tropical situation is demonstrated by rocks of Homerian age, which consist of limestones and silty mudstones containing a diverse fossil biota and bioherms. The Homerian was also a time of substantial global environmental change, associated with pronounced climate shifts, glacio-eustatic sea-level fluctuations, marine biodiversity crises (Mulde Extinction Event, *lundgreni* Event or Big Crisis) and carbon isotope

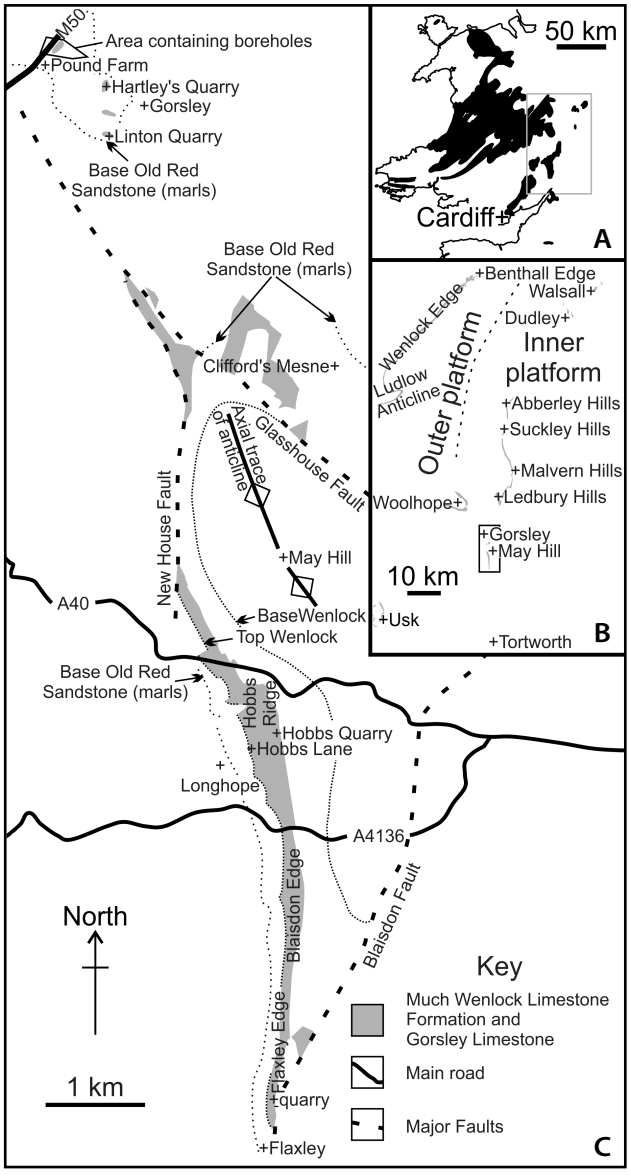

Figure 1. Location maps for the Silurian in Wales and central England showing the locations given in the text. • A – Silurian outcrops (black) in Wales and central England, with the area containing the Welsh Borders and central England highlighted. • B – outcrops of Homerian limestones (grey) upon the Midland Platform of the Welsh Borders and central England, with the study area highlighted. • C – outcrops of the Much Wenlock Limestone Formation and Gorsley Limestone (grey) situated around May Hill and Gorsley, respectively (modified from Lawson 1954, 1955). The main structural features are shown, as are the major conformable stratigraphic boundaries within the Silurian. The core of the May Hill anticline contains a Llandovery succession, the base and top of the Wenlock Series are shown, as is the base of the Old Red Sandstone, which roughly approximates to the Ludlow–Přídolí boundary.

excursions (Johnson 2006, Loydell 2007, Calner 2008, Cramer *et al.* 2012, Trotter *et al.* 2016). Many of these changes have been used as a means of correlation and age constraint. In particular, the positive double-peaked Homerian carbon isotope excursion (CIE) (informally called Mulde CIE based on equivalent strata on Gotland, Sweden) is recognised from the Midland Platform (Corfield *et al.* 1992, Fry *et al.* 2017, Ray *et al.* 2020), as well as other palaeogeographic regions including Baltica, Laurentia and peri-Gondwana (Porębska *et al.* 2004, Cramer *et al.* 2006, Calner *et al.* 2012, Frýda & Frýdová 2014, McAdams *et al.* 2018, Danielsen *et al.* 2019, Manda *et al.* 2019, Biebesheimer *et al.* 2021). The Homerian CIE is globally constrained within multiple sections by age diagnostic graptolite and conodont occurrences, and accordingly can be correlated to the geologic timescale (Fig. 2), making this CIE an important means of correlation within the Silurian (Cramer *et al.* 2012, Melchin *et al.* 2020).

The age constraint and correlation of the Homerian limestones within the May Hill and Gorsley inliers is hindered by limited exposure. Notably, the thickness and lateral extent of lithofacies is difficult to determine, as is the relationship between lithostratigraphical units, the geologic timescale and the globally recognised Homerian stage slices (Ho1 to Ho3) (Cramer *et al.* 2011). The current age model for the Much Wenlock Limestone Formation of the May Hill Inlier and its likely equivalent within the Gorsley Inlier, the Gorsley Limestone, is based upon the correlation of shelly faunas, lithological comparisons and regional stratigraphical considerations (Lawson 1954, 1955), and as such has previously been considered as loosely indicative of the Homerian (Bassett 1974, Hurst *et al.* 1978); while the Gorsley Limestone was previously considered to be possibly of Ludlow age (see Aldridge *et al.* 2000, pp. 202–204). Nonetheless, the regional correlation framework for Silurian rocks in the British Isles (Cocks *et al.* 1992) considers both lithostratigraphic units as restricted to the upper Homerian (Ho3 stage slice / *Colonograptus ludensis* graptolite Zone). Such an age assignment is based upon lithological correlation with the most deep-water expression of the Much Wenlock Limestone Formation at Wenlock Edge and the Ludlow Anticline, which contain age diagnostic graptolites (Ziegler *et al.* 1974, p. 108). However, the onset of Much Wenlock Limestone Formation deposition has been shown to be diachronous (Fig. 2), with an older base to the formation occurring within the shallower-water settings of the inner platform. Moreover, upon the northern part of the Midland Platform numerous and extensive exposures, alongside borehole records, have allowed a detailed stratigraphic framework to be established. This framework is based on correlation using lithofacies (Ratcliffe 1991, Ratcliffe & Thomas 1999), sequence stratigraphy (Ray & Butcher 2010, Ray *et al.* 2010, Coe & Ray 2022) (Fig. 2), volcanic ash (bentonite) layers (Ray *et al.* 2011, 2013), and the Homerian CIE (Corfield *et al.* 1992, Marshall *et al.* 2012, Blain *et al.* 2016, Fry *et al.* 2017, Ray *et al.* 2020), and includes sections containing a radioisotope date

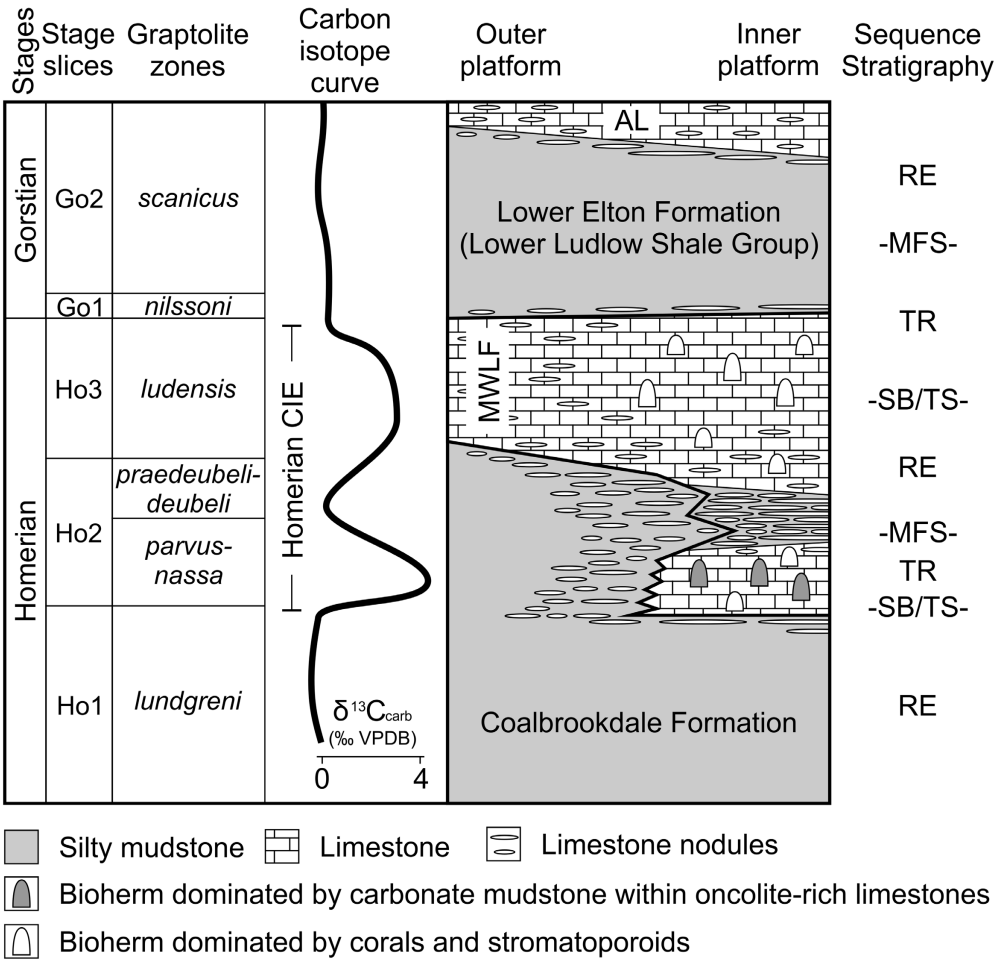

Figure 2. The relationship between the geologic timescale (Melchin *et al.* 2020), carbon isotope trends, lithostratigraphical units between the outer (*e.g.* southern Wenlock Edge and Ludlow) and inner (*e.g.* Dudley, Walsall and the Abberley, Suckley and Malvern hills) parts of the Midland Platform, and regional sequence stratigraphy. The carbon isotope curve, showing the Homerian carbon isotope excursion (CIE), is schematic and based upon regional and global curves (Fry *et al.* 2017, Melchin *et al.* 2020, Ray *et al.* 2020), and the sequence stratigraphy reflects regional and global sea-level changes (Loydell 1998, Johnson 2006, Coe & Ray 2022). Note that the Much Wenlock Limestone Formation (MWLF) of the inner platform consists of lower and upper limestones, separated by nodular beds, while the outer platform succession consists solely of an upper limestone unit. The platform-wide occurrence of mid-Ludlow (Gorstian-Ludfordian boundary) limestones are referred to here as the Aymestry Limestone (AL). Across the Midland Platform are the following sea-level changes and their bounding surfaces: RE – regression; TR – transgression; SB/TS – sequence boundary and combined transgressive surface; MFS – maximum flooding surface.

and age-diagnostic fossils, thereby allowing correlation with the geologic timescale (Cramer *et al.* 2012, Fry *et al.* 2017). Based on this framework the oldest onset of Much Wenlock Limestone Formation deposition began near the top of Ho1 (uppermost *Cyrtograptus lundgreni* graptolite Zone) within the inner platform successions of the Dudley and Walsall inliers of the West Midlands, and the Abberley, Suckley and Malvern hills, while the youngest onset began in the upperpart of Ho2 to base Ho3 (upper *Colonograptus praedeubeli–Col. deubeli* to base *Col. ludensis* graptolite zones) within the outer platform successions of Wenlock Edge and the Ludlow Anticline. Across the northern half of the Midland Platform the replacement of limestones by silty mudstones is near synchronous and corresponds to the end of the Homerian (top Ho3 / top *Col. ludensis* graptolite Zone) (Ratcliffe & Thomas 1999, Fry *et al.* 2017).

This study aims to extend knowledge of the stratigraphy of the Homerian limestones of the May Hill and Gorsley inliers, and has focused upon the identification of sections considered representative of the succession (*i.e.* Hobbs Quarry, Hobbs Lane, and Linton Quarry). From these sections we have derived new data to highlight carbon isotope excursions and indicate their interregional correlation. Notably, this study has identified the globally recognised Homerian CIE, and associated eustatic sea-level fluctuations, and time-specific facies, which have facilitated correlation with the detailed stratigraphic framework of the northern Midland Platform, and are reflective of global environmental change.

Identification of representative sites

Fieldwork within the study area of May Hill and Gorsley investigated exposures of the Much Wenlock Limestone Formation and Gorsley Limestone (Fig. 1). In particular, we visited the sites described in the Geological Conservation Review of British Silurian Stratigraphy (Aldridge *et al.* 2000), alongside many of those described by Gardiner (1920), Lawson (1954, 1955), and Ratcliffe & Thomas (1999). The initial aim was to identify extensive exposures representative of the succession, which were suitable for carbon isotope analysis, sedimentary logging, lithofacies determination and sequence stratigraphic interpretation. Having identified the most suitable sites, data collection was undertaken with the aim of improving correlation and age constraint. These sites can be located using the Ordnance Survey National Grid reference system (Hobbs Quarry SO 6949 1930; Hobbs Lane SO 6924 1928; Linton Quarry SO 6778 2567).

The Much Wenlock Limestone Formation of the May Hill Inlier occurs along a 10 km north-south trending outcrop belt, which is broken by numerous faults (Fig. 1). In the central part of the inlier (between the roads A40 and A4136), along Hobbs Ridge, the Much Wenlock Limestone Formation has an estimated thickness of 107 m, while to the south from Blaisdon Edge to Flaxley Edge the formation thins to 30 m (Lawson 1955). The thickened succession along Hobbs Ridge consists of lower and upper limestones separated by nodular beds. The limestone divisions have historically been quarried, with the resultant exposures allowing for thickness estimates of 18 m for the lower limestone (Lawson 1955, p. 89) and 2–4 m for the upper limestone (Ratcliffe & Thomas 1999, fig. 3). The three-fold division of the Much Wenlock Limestone Formation is best accessed in exposures near the village of Longhope, and these are the focus of our study. Here Hobbs Quarry, a Site of Special Scientific Interest (SSSI) and Nature Reserve, exposes the lower limestone and its transition into the overlying nodular beds (Lawson 1955, Ratcliffe & Thomas 1999; Aldridge *et al.* 2000, pp. 204, 205) (Fig. 3A). Stratigraphically higher, Hobbs Lane, a sunken path that runs between Longhope and the quarries along Hobbs Ridge, exposes the upper part of the nodular beds and the majority of the upper limestone (Fig. 3B), with the Gorstian age Flaxley Beds (part of the Lower Ludlow Shale Group) a few meters above the top of the section (Gardiner 1920, Lawson 1955). Furthermore, the upper limestone is also exposed in quarries to the immediate north of Hobbs Lane (Fig. 3C).

Within the southern half of the May Hill Inlier the upper limestone division cannot be distinguished, and the limestones commonly crop out as a white coralliferous and porous dolomite (Lawson 1955). Along Blaisdon Edge the quarries are mostly infilled, with exposures typically 0.5–1.0 m in height, and as such are unsuitable for establishing the details of the succession. At the southern end of Flaxley Edge (SO 6942 1550) is a series of more extensive exposures within abandoned quarries. However, the limestones are dolomitic, have a porous sucrosic texture and contain numerous vugs, and in this altered state are unsuitable for carbon isotope analysis. Nonetheless this faulted and overturned succession likely equates to the lower limestone and nodular beds; it begins with isolated exposures of massive limestones, which near the top of the formation give way to *c.* 10 m of limestone beds and silty mudstones.

The Gorsley Inlier exposes a small area of Silurian strata and contains four abandoned quarries, which have exposed the Gorsley Limestone in their base, and an overlying very thin and incomplete Ludlow succession (Lawson 1954, fig. 1). The Gorsley Inlier is considered to represent an area of syndepositional tectonic uplift, termed the 'Gorsley High' or 'Gorsley Axis' (Aldridge *et al.* 2000, pp. 379–381; Hillier *et al.* 2023); the geographic extent of this palaeo-bathymetric feature is best illustrated by regional Ludlow series isopach maps (see Holland & Lawson 1963). Linton Quarry, a SSSI and public open space, currently provides the best access to the Gorsley Limestone (Aldridge *et al.* 2000, pp. 202–205, 379–381), and is the focus of our study (Fig. 3D). At Linton Quarry 2.8 m of Gorsley Limestone is currently exposed, although earlier records indicated 3.6 m, and as much as 5.4 m at nearby Hartley's Quarry (Lawson 1954). Historically the Gorsley Limestone has been correlated with the mid-Ludlow Aymestry Limestone (Fig. 2), but based upon lithological, stratigraphical and palaeontological grounds the current consensus is that it correlates with the Homerian Much Wenlock Limestone Formation (Cocks *et al.* 1992). In particular, the lithology of the Gorsley Limestone has been considered essentially inseparable from that of the Much Wenlock Limestone Formation near Ledbury; it has been shown that the Aymestry Limestone regionally thins and is cut out towards the Gorsley inlier; and the shelly faunas of the Gorsley Limestone are more indicative of the Much Wenlock Limestone Formation than the Aymestry Limestone (Lawson 1954, 1955; Holland & Lawson 1963).

The most northerly exposure of the Gorsley Limestone occurs 1 km from Linton Quarry, within a valley near Pound Farm. This valley is occupied by the M50 motorway, and borehole records associated with works carried out in 1991, have been made accessible by the British Geological Survey (BGS ID268629 to 268641). Lithological descriptions for the boreholes are basic, but indicate a substantially greater thickness of Gorsley Limestone than previously described. Within the quarry near Pound Farm, boreholes penetrate the Gorsley Limestone

Figure 3. Exposures of Homerian limestones, which are representative of the succession within the May Hill and Gorsley inliers. • A – the lower limestone and nodular beds divisions of the Much Wenlock Limestone Formation at Hobbs Quarry near Longhope (SO 6949 1930). Looking west at the southern end of the main quarry face. • B – the uppermost nodular beds and upper limestone divisions of the Much Wenlock Limestone Formation at Hobbs Lane near Longhope (SO 6924 1928). Looking east at the succession outcropping in the lane side and floor. Note the hammer (30 cm length) is resting in a notch containing silty mudstone partings within more massive crinoidal grainstones. • C – the upper limestone division of the Much Wenlock Limestone Formation in a small quarry immediately north of Hobbs Lane (SO 6920 1933). Looking east, note the location of a possible iron-pan, the hammer (30 cm length) is resting in the same notch containing silty mudstone partings within more massive crinoidal grainstones, as identified in Hobbs Lane. • D – the Gorsley Limestone and overlying Lower Siltstone at Linton Quarry near Gorsley (SO 6778 2567). Looking east, and at the eastern end of the quarry, the wooden staff is 120 cm in length.

and allow for correlations with the limestones of surrounding boreholes (Fig. 1). Borehole depths range from 10–30 m, with the most extensive borehole record (ID268634; SO 6722 2666) containing at least 25.5 m of gently dipping (0–5°) Gorsley Limestone. The Gorsley Limestone is described as either argillaceous and nodular with silty mudstone partings or as silty mudstones with argillaceous limestone nodules. In both lithofacies the maximum size of the nodules is notable (diameter of up to 256 mm) and resembles that seen at Linton Quarry. The silty mudstones with limestone nodules typically occur below the nodular limestones, and within the most extensive borehole record, these lithofacies represent 13.6 m and 11.9 m, respectively. However, the thickness

of the nodular limestones at the top of the Gorsley Limestone is variable (absent to 17.6 m), but it is unclear how much of this variation is the result of truncation by the modern or Silurian land surface, as opposed to local lithofacies variability or the inconsistent assignment of lithofacies.

Field and laboratory methods

Sedimentary logging of each section was undertaken and samples for carbon isotope analysis were collected at 0.20 m intervals, alongside a limited number of thin sections taken to further investigate lithofacies and diagenesis (Tab. 1). From each sample 2000 µg of carbonate rock powder was prepared. This method of analysing bulk rock for stable isotopes, which inevitably contains some skeletal material, has been shown to provide reliable results in other Silurian studies (*e.g.* Cramer *et al.* 2006, Ray *et al.* 2020). At the British Geological Survey Stable Isotope Facility, the sample material was weighed into Exetainer vials to provide ~400 µg of carbonate. The septa-sealed vials were loaded into an Elementar iso FLOW headspace analyser, which automatically flushes each vial with helium and injects anhydrous phosphoric acid to react with the carbonate to liberate CO_2 gas. The vials were left overnight to react at 50 °C. Sample gas was then transferred online via a continuous flow of helium to an Elementar isoprime precisION isotope ratio mass spectrometer for oxygen and carbon isotope analysis. Isotope values are reported in delta (δ) notation as per mille (‰) variations of the $^{13}C/^{12}C$ and $^{18}O/^{16}O$ ratios relative to the Vienna Pee Dee Belemnite (VPDB) international reference delta scale. Isotope data were calibrated to the VPDB scale using a laboratory Carrara marble standard. An external precision of better than 0.1‰ has typically been achieved for both $\delta^{13}C$ and $\delta^{18}O$. In total, 75 samples provided results and carbon isotope curves have been produced, alongside sedimentary logs, for Hobbs Quarry, Hobbs Lane, and Linton Quarry (Fig. 4).

Carbon isotope results

At Hobbs Quarry $\delta^{13}C_{carb}$ values range between 2.94‰ and 4.39‰. Within the lower 3.8 m values decline upsection from above to below 4‰, and this decline in values corresponds to the transition between the lower limestone and nodular beds divisions of the Much Wenlock Limestone Formation. Within the upper 1.0 m of the section there is a notable rebound in values to between 3.59–4.09‰. In addition, two samples of carbonate mudstone collected from within the nearest bioherm provide

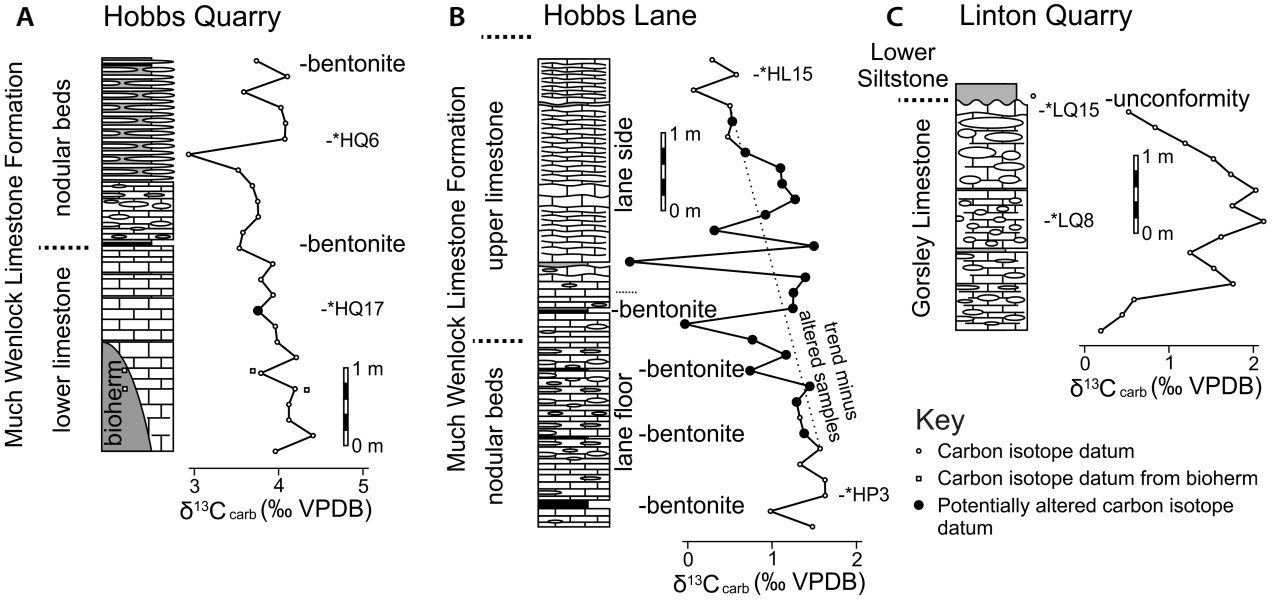

Figure 4. Sedimentary logs and $\delta^{13}C_{carb}$ values from Homerian limestones, which are representative of the succession within the May Hill and Gorsley inliers. $\delta^{13}C_{carb}$ values considered as unaltered are given as open circles, while potentially altered samples are solid circles. Note potentially altered samples have been identified by their associated oxygen isotopic values. Values above −4‰ are considered anomalously high and reflective of the alteration of the primary oxygen isotopic signal. Legend: * – position and sample code of thin sections shown in Fig. 5. • A – Hobbs Quarry (SO 6949 1930), note the squares are unaltered $\delta^{13}C_{carb}$ values from within the bioherm. • B – Hobbs Lane (SO 6928 1928 to SO 6924 1928), note limestones crop out in the lane side and floor for *c.* 40 m. • C – Linton Quarry (SO 6778 2567), note the single $\delta^{13}C_{carb}$ value from the Ludfordian Lower Siltstone. For further explanation of the logs see the key in Fig. 2, and descriptions in the text.

Table 1. $\delta^{13}C_{carb}$ and $\delta^{18}O_{carb}$ values from Hobbs Quarry, Hobbs Lane, and Linton Quarry. Legend: * – thin section analysis to investigate lithofacies and diagenesis.

Hobbs Quarry			
Sample code [bedded strata (HQ) and bioherm (B)]	Position from lowest sample (m)	$\delta^{13}C_{carb}$	$\delta^{18}O_{carb}$
HQ26	0.0	3.95	–6.17
HQ25	0.2	4.39	–4.29
HQ24	0.4	4.11	–5.43
HQ23	0.6	4.11	–4.92
HQ22	0.8	4.18	–4.84
HQ21*	1.0	3.78	–4.73
HQ20	1.2	4.20	–4.32
HQ19	1.4	3.97	–5.20
HQ18	1.6	3.95	–4.41
HQ17*	1.8	3.75	–3.73
HQ16	2.0	3.93	–4.31
HQ15	2.2	3.78	–4.88
HQ14	2.4	3.92	–4.31
HQ13	2.6	3.53	–4.90
HQ12	2.8	3.57	–4.36
HQ11	3.0	3.75	–4.73
HQ10*	3.2	3.75	–5.00
HQ9	3.4	3.68	–5.63
HQ8	3.6	3.52	–4.82
HQ7	3.8	2.94	–4.35
HQ6*	4.0	4.06	–5.87
HQ5	4.2	4.07	–4.72
HQ4	4.4	4.02	–5.24
HQ3	4.6	3.59	–5.18
HQ2	4.8	4.09	–5.23
HQ1	5.0	3.73	–5.50
B1	0.6	4.34	–6.34
B7	1.2	3.68	–5.51
Hobbs Lane			
Sample code [path floor (HP) and lane side (HL)]	Position from lowest sample (m)	$\delta^{13}C_{carb}$	$\delta^{18}O_{carb}$
HP1	0.0	1.47	–6.67
HP2	0.2	0.98	–5.37
HP3*	0.4	1.62	–5.96
HP4	0.6	1.62	–5.28
HP5	0.8	1.33	–5.09
HP6	1.0	1.56	–5.48
HP7	1.2	1.37	–2.89
HP8	1.4	1.32	–4.24
HP9	1.6	1.28	–2.27
HP10	1.8	1.44	–1.82
HP11	2.0	0.74	–1.78
HP12	2.2	1.17	0.91
HP13	2.4	0.76	–0.02
HP14	2.6	–0.03	0.20
HP15*	2.8	1.24	–0.48
HL1*	3.0	1.25	1.16
HL2	3.2	1.39	1.08
HL3	3.4	–0.70	–0.16
HL4	3.6	1.49	0.95
HL5	3.8	0.32	0.21
HL6	4.0	0.92	0.62
HL7	4.2	1.27	1.01
HL8	4.4	1.11	0.79
HL9	4.6	1.09	1.37
HL10	4.8	0.68	–0.76
HL11	5.0	0.47	–4.07
HL12	5.2	0.53	–2.88
HL13	5.4	0.50	–5.28
HL14	5.6	0.07	–6.74
HL15*	5.8	0.58	–7.55
HL16	6.0	0.27	–6.87
Linton Quarry			
Sample code	Position from lowest sample (m)	$\delta^{13}C_{carb}$	$\delta^{18}O_{carb}$
LQ1	0.0	0.15	–7.02
LQ2	0.2	0.41	–6.98
LQ3	0.4	0.55	–5.71
LQ4*	0.6	1.75	–6.01
LQ5	0.8	1.51	–7.00
LQ6	1.0	1.23	–5.32
LQ7	1.2	1.60	–4.89
LQ8*	1.4	2.12	–5.12
LQ9	1.6	1.74	–6.17
LQ10	1.8	2.02	–4.95
LQ11	2.0	1.72	–4.87
LQ12*	2.2	1.51	–4.71
LQ13	2.4	1.17	–4.65
LQ14	2.6	0.81	–4.68
LQ15*	2.8	0.49	–4.61
LQ16	3.0	–0.65	–7.96

values (4.34‰ and 3.68‰) similar to the adjacent bedded strata (Fig. 4A). Alteration identifiable from the isotopic signal is restricted to a single datum containing an anomalously high oxygen isotopic value (see discussion below). Thin sections mostly show primary textures, although spar filled cavities that contain both marine and meteoric cements, indicate alteration during multiple phases of diagenesis (Fig. 5). However, as spar filled cavities were avoided in the collection of carbonate rock powder, the resulting isotopic values likely reflect a primary signal.

At Hobbs Lane $\delta^{13}C_{carb}$ values range between −0.70‰ and 1.62‰. Overall values decline up-section from above to below 1‰, with negative values associated with two isolated samples, which are not reflective of the broad trend. Oxygen isotopic values range between −7.55‰ and 1.37‰, and within the middle of the section are considered

anomalously high (above −4‰) for the Wenlock of the Midland Platform (*e.g.* Hughes & Ray 2016, Ray *et al.* 2020). Furthermore, thin sections from this interval show euhedral to subhedral dolomite replacing calcite cements. Accordingly, the anomalous oxygen isotopic values and dolomitization likely reflect a narrow interval of diagenetic alteration (see example in Jenkyns 1995), which may be linked to the movement of groundwater, as evidenced by the local redeposition of iron oxides to form an iron-pan (Fig. 3C). However, the omission of carbon isotope data from the middle of the section does not prevent recognition of the overall decline in values and shows that a primary carbon isotopic signal persists. Note that the alteration may only unduly affect the oxygen isotopic values, but not the carbon isotope values (Fig. 4B, Tab. 1).

At Linton Quarry within the Gorsley Limestone $\delta^{13}C_{carb}$ values range between 0.15‰ and 2.12‰. Values show a sawtooth rise to a peak within the middle of the section, before declining towards the unconformity. A single value from the base of the overlying Lower Siltstone has notably lower carbon and oxygen isotopic values (−0.65‰, −7.96‰, respectively), and thereby highlights the difference in lithology and age across the unconformity surface (Fig. 4C). Although there is no obvious evidence of alteration from the isotopes, thin sections from the upper half of the Gorsley Limestone show dissolution, secondary porosity, and multiple phases of diagenesis, including meteoric cements and localised dolomitization (Fig. 5). These features are indicative of the karstification of the unconformity surface (Hillier *et al.* 2023, p. 2018), and as such the declining $\delta^{13}C_{carb}$ values towards the unconformity may be overprinted by a meteoric influence on the succession (see example in Calner *et al.* 2010). Nonetheless, as diagenesis typically acts to lower $\delta^{13}C$ values (Cramer & Jarvis 2020), the rise and peak in values within the Linton Quarry curve must reflect elevated and rising primary $\delta^{13}C_{carb}$ values, irrespective of the influence of diagenesis.

Correlation based upon the Homerian carbon isotope excursion

The Homerian CIE is recognised from a variety of marine depositional settings across the Midland Platform. These range from the shallow-water reefal successions of the Much Wenlock Limestone Formation of the Dudley inliers, northern Wenlock Edge, and the Malvern and Suckley hills, to the deeper-water platform marginal limestones and silty mudstones of the Much Wenlock Limestone Formation and underlying Coalbrookdale Formation at the southern end of Wenlock Edge, and within the Ludlow Anticline (Fry *et al.* 2017, Ray *et al.* 2020). A comparison of $\delta^{13}C_{carb}$ values shows clear spatial variations, with lighter values recorded from more distal settings and heavier values from shallower settings (Blain *et al.* 2016, Ray *et al.* 2020). Furthermore, it has been shown that regional differences in the rate of palaeo-bathymetric change and the nature of the associated carbonates could control and offset the broad trend in isotopic values (Ray *et al.* 2020). Nonetheless trends in $\delta^{13}C_{carb}$ values persist and form the basis of global correlation. In particular, the first peak of the double-peaked Homerian CIE typically begins near the Ho1–Ho2 stage slice boundary and is restricted to the Ho2, while the second peak begins in Ho2 and ends near to the Homerian–Gorstian boundary (Ho3–Go1) (Fry *et al.* 2017) (Fig. 2). In terms of magnitude the first peak is almost always slightly larger than the second peak (Manda *et al.* 2019), and this is the case upon the Midland Platform. Comparison between the double-peaks of the Dudley inliers (shallowest setting) and the Malvern and Suckley hills (slightly deeper setting) give maximum values of 5.5‰ and 4.8‰ for the first peak, and 3.8‰ and 3.0‰ for the second peak (Ray *et al.* 2020). Given the local variability in the magnitude and shape of the Homerian CIE, the carbon isotope curves from the May Hill and Gorsley inliers are most likely to be similar to the curve derived from the Malvern and Suckley hills (Fig. 6). Here the Homerian CIE is identified within two closely spaced sections (2.5 km apart) and is the nearest Homerian CIE curve to the Gorsley and May Hill inliers (25–30 km north of the current study area). In addition, palaeogeographic studies indicate north-south trending palaeo-bathymetric contours (Hurst *et al.* 1978) suggesting a similar depositional setting; as is reflected by the threefold division of the Much Wenlock Limestone Formation into the lower and upper limestones separated by nodular beds at May Hill, and the Lower and Upper Quarried Limestone members separated by the Nodular Beds Member within the Malvern and Suckley hills (Lawson 1955, Ray *et al.* 2013).

In summary, the carbon isotope trends and values derived from Hobbs Quarry, Hobbs Lane, and Linton Quarry correspond to intervals within the Homerian CIE (Figs 4 and 6). At Hobbs Quarry the occurrence of values above 4‰ indicate the first peak of the Homerian CIE, and the decline in values indicates the falling limb of this peak. In addition, comparison with the curve from the Malvern and Suckley hills identifies a good-fit with the entirety of the Hobbs Quarry curve, including the minor positive rebound in values near the top of the section. At Hobbs Lane the presence of declining values below a unit of likely Gorstian age (the Flaxley Beds) is indicative of the falling limb of the second peak and the end of the Homerian CIE. It is of note that, while the overall shape of the curve is like that from the Malvern and Suckley hills, the values from Hobbs Lane are in the order of 1‰ lower.

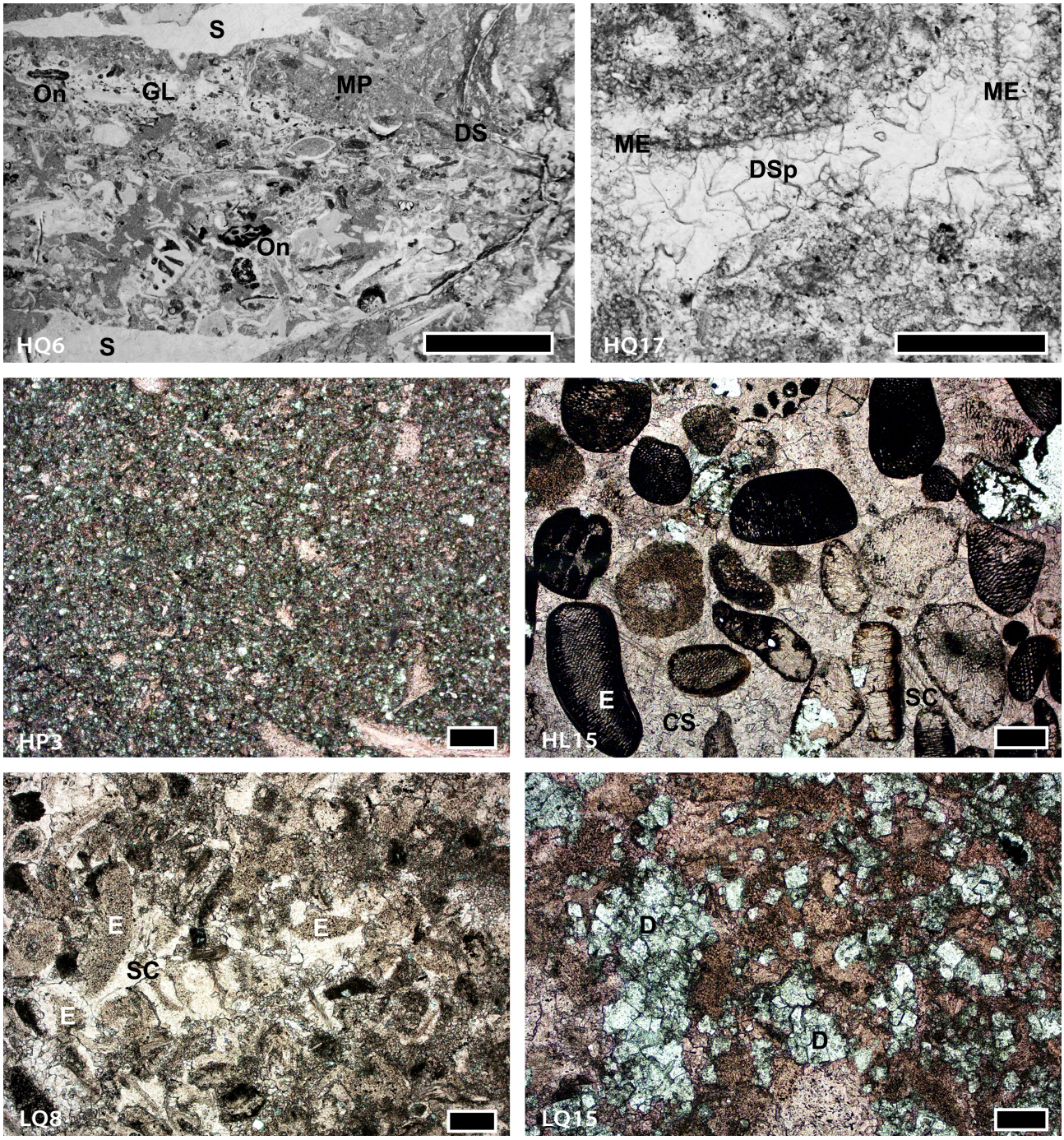

Figure 5. Thin section photographs, not orientated with respect to way up, showing textures and diagenetic features, stained with alizarin red S and potassium ferricyanide. See Fig. 4 and Tab. 1 for the stratigraphic position of the thin sections. It should be noted that the diagenetic features shown (*e.g.* dissolution seams, drusy and syntaxial cements, dolomitization) could form in multiple diagenetic environments, including a meteoric one. Accordingly, our interpretation of meteoric diagenesis is, in part, informed by the wider geological context, including the occurrence of an unconformity, and probable episodes of subaerial exposure. • HQ6 – Hobbs Quarry sample demonstrating various textures and diagenetic features including mudstone-packstone portions (MP), adjacent to grainstone lenses (GL) with oncolite (On) coated grains (dark grey coating of grains such as gastropods, brachiopods, crinoids, and corals). Later spar-filled cavities (S) and dissolution seams (DS) were avoided in isotope sampling. Scale bar = 5 mm. • HQ17 – Hobbs Quarry sample showing the detail of a drusy spar-filled (DSp) cavity (meteoric diagenesis), with adjacent micrite envelopes (ME) (early marine diagenesis) identified by the very fine lines of micrite marking the former position of the edge of grains. Scale bar = 250 µm. • HP3 – Hobbs Lane sample of mudstone-wackestone, typical of the nodular beds. Scale bar = 200 µm. • HL15 – Hobbs Lane sample from the upper limestone showing iron-stained grainstone, mainly echinoderm bioclasts (E) with calcite spar (CS), some of which is syntaxial on echinoderm bioclasts (SC). Scale bar = 200 µm. • LQ8 – Linton Quarry sample showing syntaxial calcite (SC) cements overgrown on echinoderm bioclasts (E) of a likely meteoric origin. Scale bar = 200 µm. • LQ15 – Linton Quarry sample of a heavily dolomitized (D) packstone from immediately below the unconformity surface. Scale bar = 200 µm.

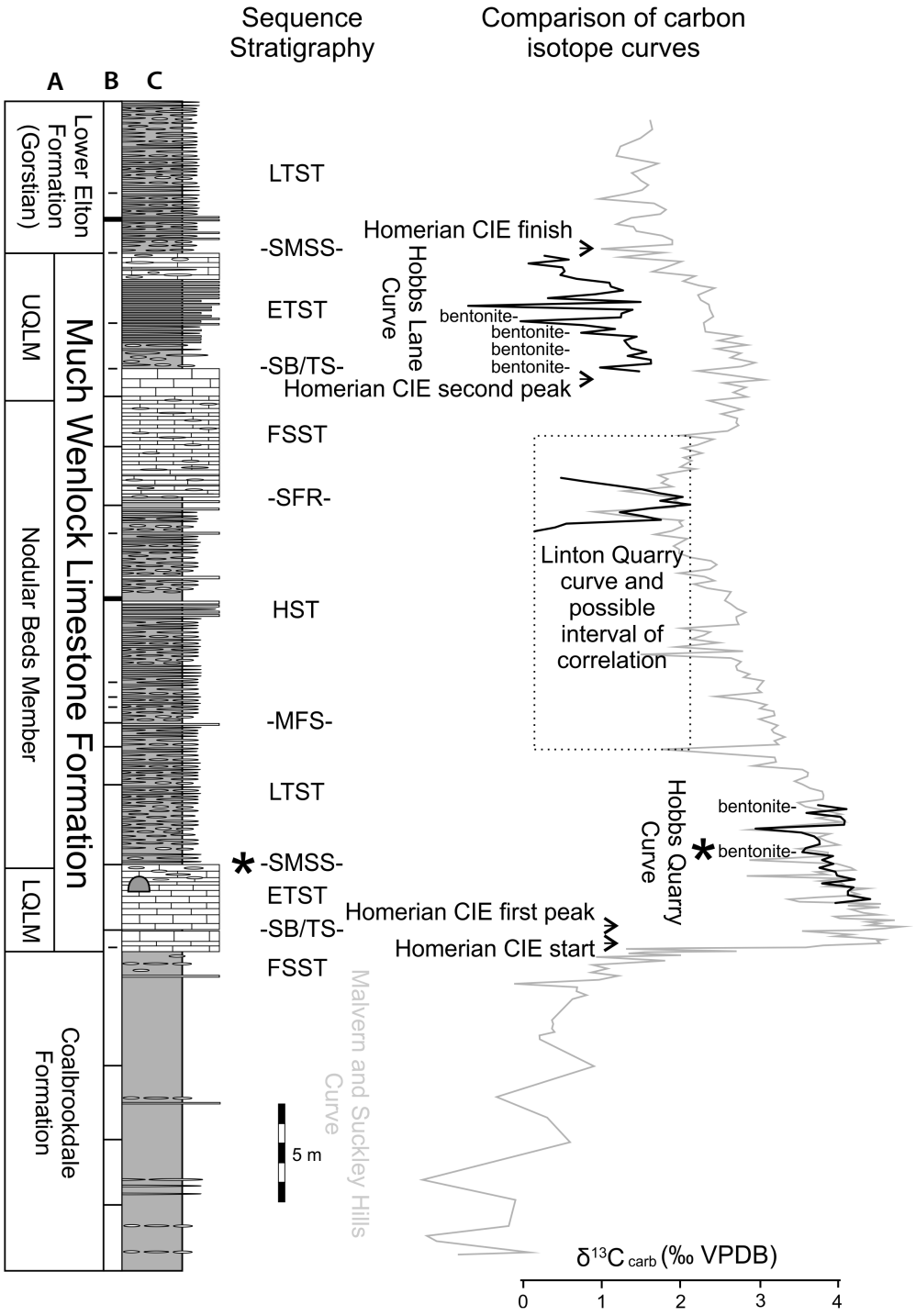

Figure 6. A comparison of the carbon isotope curve from the Malvern and Suckley hills (from Whitman's Hill Quarry and Bruff Business Park Section, modified from fig. 6, Ray *et al.* 2020), with the curves from Hobbs Quarry, Hobbs Lane, and Linton Quarry. • A – lithostratigraphy of the Malvern and Suckley hills; LQLM – Lower Quarried Limestone Member; UQLM – Upper Quarried Limestone Member. • B – distribution of bentonites within the Malvern and Suckley hills; dashed line indicates minor bentonites (< 2 cm); thin line indicates prominent bentonites (> 2 to < 10 cm); thick line indicates very prominent bentonites (> 10 cm). Legend: * – bentonite WH5 and a similarly positioned bentonite at Hobbs Quarry. • C – sedimentary log of the uppermost Coalbrookdale Formation, Much Wenlock Limestone Formation, and lowermost Lower Elton Formation within the Malvern and Suckley hills. For further explanation of the log see the key in Fig. 2, and descriptions in Ray *et al.* (2013, 2020). Within the Malvern and Suckley hills are the following systems tracts and their bounding surfaces: SB/TS – sequence boundary and combined transgressive surface; ETST – early transgressive systems tract; SMSS – surface of maximum sediment starvation; LTST – late transgressive systems tract; MFS — maximum flooding surface; HST – highstand systems tract; SFR – surface of forced regression; FSST – falling stage systems tract.

Comparable differences in values are also reported from closely-spaced (*c*. 9 km between Benthall Edge Quarry and Lea South Quarry) shallow-water reefal successions within the uppermost Homerian at the northern end of Wenlock Edge. There, these differences are considered to reflect local variations in water depth, and carbonate provenance and productivity, which are characteristic features of the onset of transgression into the overlying Gorstian (Ray *et al.* 2010, Blain *et al.* 2016, Fry *et al.* 2017). Lastly, peak values within the Linton Quarry curve are above those typically expected from pre- or post-excursion strata (Figs 2, 6), and accordingly appear to show values down or up slope from the peak values of the Homerian CIE. In addition, a Gorstian age seems unlikely for the Gorsley Limestone, as this interval contains no globally recognised carbon isotopic excursions. A weak, and locally expressed, $\delta^{13}C_{carb}$ excursion is reported from near the Gorstian-Ludfordian boundary of Baltica (Linde CIE) but this seems a speculative match, as its maximum reported magnitude (1.4‰) is too small to be traced with confidence, and the peak values are less than that reported from Linton Quarry (Samtleben *et al.* 2000, Kaljo & Martma 2006, Cramer *et al.* 2011). Using these preliminary carbon isotopic correlations as a starting point, the sedimentology, lithofacies, and sequence stratigraphy of the sections can now be considered as a means of further refining age and correlation.

Stratigraphy of Hobbs Quarry, May Hill Inlier

The Hobbs Quarry succession shows an upward fining of the limestones, with crinoidal grainstones passing upwards into skeletal and oncoidal packstones and wackestones, and carbonate mudstones, a transition that is accompanied by an increase in silty mudstones as limestone beds are less continuous and more nodular up section. The limestones are rich in crinoids, bivalves, brachiopods, corals, and bryozoans, as well as clumps of microbial calcifying cyanobacteria (e.g. *Girvanella* and *Rothpletzella*) and oncolitic structures (Fig. 5), and are accompanied by bioherms in the lower half of the quarry face. The succession reflects a transgression, which at Hobbs Quarry can be subdivided into three retrogradational parasequences, and across the inlier is marked by the replacement of the lower limestone by the nodular beds (Lawson 1955). In terms of lithofacies the lower limestone and nodular beds divisions correspond to the thick bedded oncolite-rich and nodular limestone lithofacies, respectively; with the transition between these lithofacies characteristic of the interbedded limestone and silty mudstone lithofacies (Ratcliffe 1991, Ratcliffe & Thomas 1999). The boundary between the divisions is marked by a change from bedded to nodular limestones, and coincides with the occurrence of a prominent (6 cm thick) bentonite horizon (Figs 3A, 4A). Eight bioherms, two of which are identifiable by an arching of overlying strata in places where no bioherm is exposed, occur at regular intervals along the quarry face (*c.* 8 m between the cores of adjacent bioherms). The bioherms are dominated by carbonate mudstone, with a secondary contribution from crinoids near their base (Ratcliffe & Thomas 1999) and are restricted to the thick bedded oncolite-rich lithofacies. Bioherm growth terminates (*c*. 1.2 m below the top of the lower limestone division) as thick amalgamated limestone beds give way to medium to thin beds with silty mudstone partings (the transitional interbedded limestone and silty mudstone lithofacies). The end of bioherm growth and change in lithofacies reflects transgression and a drowning of the carbonate system.

The carbon isotope curve from Hobbs Quarry is indicative of the falling limb of the first peak of the Homerian CIE, and corresponds to the Ho2 stage slice. Notably, the isotopically equivalent interval within the Malvern and Suckley hills is also associated with a marked transgression and the replacement of the thick bedded oncolite-rich lithofacies by the nodular limestone lithofacies. Across the interior of the Midland Platform this transgression is documented by the transition from the Lower Quarried Limestone Member to the Nodular Beds Member (Ratcliffe & Thomas 1999; Ray *et al.* 2010, 2020), while on Gotland (Sweden) this transgression is associated with a 16-m rise in sea level (sea-level event 5a from Johnson (2006)) related to the drowning of a rocky palaeoshoreline (Calner & Säll 1999). More widely the occurrence of microbial sediments such as oncolite-rich limestones, and carbonate mudstone dominated bioherms, constitute a time-specific facies (see examples in Brett *et al.* 2012), which reflect an interval of environmental change associated with the first peak of the Homerian CIE, the Mulde Extinction Event and the accompanying eustatic transgression (Calner 2005, 2008; Cramer *et al.* 2012). Within the interior of the Midland Platform, carbonate mudstone bioherms in association with oncolite-rich limestones, are reported from the Lower Quarried Limestone Member of the Dudley and Walsall inliers, and the Malvern Hills (Ratcliffe & Thomas 1999, Päßler *et al.* 2014), and are age equivalent to the bioherms at Hobbs Quarry. Lastly, within the Malvern, Suckley and Abberley hills a prominent (3–5 cm thick) bentonite horizon (WH5) at the base of the Nodular Beds Member has been traced between quarries (Ray *et al.* 2013), and appears stratigraphically equivalent to the prominent bentonite at the base of the nodular beds division at Hobbs Quarry, thereby suggesting the presence of a regionally traceable (42 km between the most distant quarries) volcanic ash horizon.

Stratigraphy of Hobbs Lane, May Hill Inlier

The Hobbs Lane succession shows an upward coarsening of the limestones from carbonate mudstones, to skeletal wackestones and packstones, to coarse grained ferruginous crinoidal grainstones (Fig. 5). Some beds contain in situ corals, while others are crowded with large isolated crinoid ossicles, or contain an abundance of the brachiopod *Atrypa reticularis*. Within the lower part of the section the limestones are typically nodular to planar bedded and are separated by silty mudstones, as well as four bentonites, the lowest of which is *c*. 10 cm thick. Within the upper part of the section the limestones become more massive, are occasionally rippled, and weather to reveal irregular flaggy beds. Thin silty mudstones separate the flaggy beds, and occur as rip-up clasts. This change in lithology and bedding reflects a shallowing, which equates to the transition from the upper part of the nodular beds division to the upper limestone division (Lawson 1955). In terms of lithofacies the succession corresponds to the nodular limestone lithofacies overlain by the ferruginous crinoidal grainstone lithofacies (Ratcliffe 1991, fig. 15). The boundary between these divisions/lithofacies is gradational, but has been placed at a level above which crinoidal grainstones become common (Figs 3B, 4B).

The carbon isotope curve from Hobbs Lane is indicative of the falling limb of the second peak and the end of the Homerian CIE, and corresponds to the Ho3 stage slice near to the Homerian–Gorstian boundary. As at Hobbs Lane, the uppermost Homerian across much of the Midland Platform is associated with regression, and the eventual widespread deposition of crinoidal grainstones. In detail the crinoidal grainstones are indicative of peak shallowing, and the onset of transgression; prior to the major transgression in the Gorstian (Ray *et al.* 2010, 2013). The switch from regression to transgression has, elsewhere on the Midland Platform, been identified by the correlation and interpretation of parasequence stacking patterns from closely spaced sections (Ray *et al.* 2010, 2013). However, within the May Hill Inlier the limited exposure prevents this approach. The ferruginous crinoidal grainstone lithofacies reflects a similar depositional setting to the crinoidal grainstone lithofacies, but is restricted to an area encompassing the Ledbury Hills and May Hill Inlier (Ratcliffe & Thomas 1999, fig. 8). Within the late Llandovery marine sedimentary rocks enriched in syndepositional iron are widespread, have been termed a time-specific facies, and linked to global processes (*e.g.* Cotter & Link 1993, Loydell 1998, Brett *et al.* 2012, McLaughlin *et al.* 2012). However, similar iron-rich facies are not widely reported from the Homerian, and accordingly where developed are more likely a reflection of local processes. In their interpretation of this lithofacies Ratcliffe & Thomas (1999) attributed its red colour to the weathering of iron oxide cements, which predated early marine cements and sediment lithification. Furthermore, it was suggested that the iron originated from the weathering of pyrite contained within the underlying nodular limestone lithofacies, either as a result of subaerial exposure or frequent submarine reworking (Ratcliffe & Thomas 1999). As the Gorsley High, with its karstic unconformity at the top of the Gorsley Limestone, and presumably frequently reworked fringing sediments, occurs near the geographic centre of ferruginous crinoidal grainstone deposition, it seems a good candidate for the source of iron.

Stratigraphy of Linton Quarry, Gorsley Inlier

The Linton Quarry succession consists of nodular wackestones, packstones, and grainstones containing crinoids, brachiopods, and corals, as well as clumps of microbial calcifying cyanobacteria (e.g. *Girvanella*) and oncolitic structures. Silty mudstones occur as irregular laminae that separate the nodules, and as occasional beds. The nodules near the base of the section are subspherical (3–4 cm) and locally coalesce to form elongate (8–30 cm) beds. Towards the top of the section the nodules become more irregular and larger (up to 16 cm in depth by 60 cm long) and at the top of the Gorsley Limestone form an irregular unconformity surface. In terms of lithofacies the Linton Quarry section most closely resembles the nodular beds lithofacies (Ratcliffe & Thomas 1999), with the large irregular nodules at the top of the section reflective of enhanced diagenesis and karstification in response to the development of the unconformity (Fig. 5). However, grainstones and microbial calcifying cyanobacteria are atypical components of the nodular beds lithofacies, and indicate a slightly shallower depositional setting, like the transitional succession developed above the thick bedded oncolite-rich lithofacies at Hobbs Quarry. Accordingly, the Gorsley Limestone represents a low energy environment within the photic zone, which being near the lower limit of storm wave-base, was subject to sporadic turbulence.

Comparison with borehole records show that the Gorsley Limestone at Linton Quarry represents part of at least 25.5 m of limestone nodules and likely correlates to a comparable thickness of this lithology elsewhere. Across the interior of the Midland Platform this lithology corresponds to the Nodular Beds Member of the Much Wenlock Limestone Formation, and the nodular beds division of the May Hill Inlier. Furthermore, while the revised minimum thickness for the Gorsley Limestone approximates to the regional thickness of the Nodular Beds Member (23 m to 31 m, Ray *et al.* 2010, 2013) and the poorly constrained thickness of the nodular beds division at May Hill (≤ 87 m along Hobbs Ridge), the

mid-Ludlow Aymestry Limestone, which has historically been correlated with the Gorsley Limestone (see Lawson 1954), is unlikely to have achieved this thickness within the Gorsley Inlier. Notably, the Aymestry Limestone is 12 m and 8 m thick between 7 km and 10 km (Bodenham and Clencher's Mill, respectively) to the north of Linton Quarry, and is absent and replaced by an unconformity throughout the May Hill Inlier and within sections 4.5 km and 3 km (Whittocks End and Clifford's Mesne, respectively) to the north and south of Linton Quarry (Lawson 1954, 1955; Squirrell & Tucker 1960; Holland & Lawson 1963; Phipps & Reeve 1967). Accordingly, the minimum thickness and lithology adhere to the consensus view that the Gorsley Limestone correlates with the Homerian Much Wenlock Limestone Formation.

The carbon isotope curve from Linton Quarry, alongside its association with at least 25.5 m of nodular limestones, corresponds to the low in isotopic values between the peaks of the Homerian CIE, which occurs within the Nodular Beds Member of the inner part of the Midland Platform (Ray *et al.* 2020) (Fig. 6). Similarly, the identification of the falling limbs of the first and second peaks of the Homerian CIE within the lower and upper limestone divisions of the nearby May Hill Inlier, indicates that the low in isotopic values likely occurs within the intervening nodular beds division. Assuming the Gorsley Limestone correlates to the nodular beds division, it is notable that the upper limestone is absent from the Gorsley Inlier. Accordingly, the unconformity at the top of the Gorsley Limestone not only omits the upper part of the limestone succession and the shallowest water setting, but may correspond to the surface of latest Homerian subaerial exposure and weathering, that acted as the source of iron for the ferruginous crinoidal grainstone lithofacies of the Ledbury Hills and May Hill Inlier. Furthermore, as the nodular limestones at Gorsley do not exhibit the extreme thinning observed in the Ludlow succession, it seems likely that the tectonic uplift that formed the Gorsley High began towards the end of nodular limestone deposition, within the latest Homerian.

Conclusion: a summary of the Homerian stratigraphy of the May Hill and Gorsley inliers

Carbon isotope trends and values identify the falling limbs of the first and second peaks of the Homerian CIE at Hobbs Quarry and Hobbs Lane, respectively, and the low between these peaks at Linton Quarry (Fig. 6). Comparison with the carbon isotope curve and the associated lithostratigraphy, lithofacies and sequence stratigraphy from the inner part of the Midland Platform (*i.e.* Dudley inliers, and the Malvern and Suckley hills), show substantial agreement with what has been documented from the May Hill and Gorsley inliers. Notably, the threefold division of the Much Wenlock Limestone Formation into the lower and upper limestones separated by nodular beds in the May Hill Inlier, mirrors the three members of the Much Wenlock Limestone Formation (*i.e.* Lower and Upper Quarried Limestone members separated by the Nodular Beds Member) described from the inner part of the Midland Platform, and indicates synchronicity, with limestone deposition beginning near the top of stage slice Ho1 and ending near the top of Ho3; rather than being restricted to Ho3 as previously inferred (Cocks *et al.* 1992). At Hobbs Quarry the correlation of the succession is further aided by the occurrence of microbially mediated oncolite-rich limestones and bioherms, which are a widely recognised time-specific facies of the first peak of the Homerian CIE and the accompanying Mulde Extinction Event and transgression (Calner 2008). Furthermore, a prominent bentonite situated at the base of the nodular beds division at Hobbs Quarry appears stratigraphically equivalent to a regionally traceable bentonite within the Malvern, Suckley and Abberley hills (Ray *et al.* 2013).

The carbon isotope values from Linton Quarry, alongside the lithofacies and a substantial increase in the estimated thickness of the Gorsley Limestone (from 5.4 m to 25.5 m), further support the lithological, stratigraphical, and palaeontological evidence for correlation with the Much Wenlock Limestone Formation (Lawson 1954), and suggest an age equivalence with the nodular beds, which are developed within the middle of the formation. A notable feature of the May Hill and Gorsley inliers is the localised absence of the ferruginous upper limestone division from the north and south of the study area. In the Gorsley Inlier it seems likely that the area was subject to tectonic uplift (to form the Gorsley High), subaerial exposure and weathering during the latest Homerian, and was the source of iron within the ferruginous crinoidal grainstone lithofacies of the Ledbury Hills and May Hill Inlier. In the south of the May Hill Inlier, along Blaisdon Edge and Flaxley Edge, the upper limestone division is also absent, and the Much Wenlock Limestone Formation is altered (*i.e.* dolomitic and vuggy) and reduced in thickness. Localised variations in thickness are also evident from the lower Wenlock Woolhope Limestone Formation of the same area (Lawson 1955), and may suggest variability in palaeo-bathymetry. Accordingly, the southern part of the May Hill Inlier may have been subject to subaerial exposure and weathering, but unlike within the Gorsley Inlier, the occurrence of an overlying thicker and more complete Ludlow succession (Lawson 1955, fig. 4), provides argument for more limited episodes of subaerial exposure; perhaps driven by eustatic regressions and transgressions, rather than the tectonic uplift inferred for the Gorsley Inlier.

Acknowledgements

This paper is dedicated to Jiří Kříž, a world-renowned palaeontologist and stratigrapher. The Herefordshire and Worcestershire Earth Heritage Trust assisted in identifying landowners and obtaining access and appropriate permissions for key sections. Natural England, Hobbs Nature Reserve Trust, and Linton Parish Council are thanked for granting permission for us to undertake the work. David Green is thanked for advice on the location of instructive sections within the May Hill Inlier. Borehole records from the Gorsley Inlier were made available through the British Geological Survey OpenGeoscience data, and accordingly our interpretation contains British Geological Survey materials © UKRI 2025. Melanie Leng and the British Geological Survey Stable Isotope Facility are acknowledged for the analysis and timely delivery of oxygen and carbon isotope results as part of Georgia Hazeldine's MSci research project. Paul Hands is thanked for preparing the thin sections. We are grateful for the constructive reviews given by Markes E. Johnson, Stanislava Vodrážková, and an anonymous reviewer.

References

Aldridge, R.J., Siveter, Da., Siveter, De., Lane, P.D., Palmer, D.G. & Woodcock, N.H. 2000. *British Silurian Stratigraphy*. 542 pp. Geological Conservation Review Series 19. Joint Nature Conservation Committee, Peterborough.

Bassett, M.G. 1974. Review of the stratigraphy of the Wenlock Series in the Welsh Borderland and South Wales. *Palaeontology 17(4)*, 745–777.

Bassett, M.G., Bluck, B.J., Cave, R., Holland, C.H. & Lawson, J.D. 1992. Silurian, 17–56. *In* Cope, J.C.W., Ingham, J.K. & Rawson, P.F. (eds) *Atlas of Palaeogeography and Lithofacies*. *Geological Society London, Memoir 13*. DOI 10.1144/GSL.MEM.1992.013.01.07

Biebesheimer, E.J., Cramer, B.D., Calner, M., Barnett, B.A., Oborny, S.C. & Bancroft, A.M. 2021. Asynchronous $\delta^{13}C_{carb}$ and $\delta^{13}C_{org}$ records during the onset of the Mulde (Silurian) positive carbon isotope excursion from the Altajme core, Gotland, Sweden. *Chemical Geology 576*, 120256. DOI 10.1016/j.chemgeo.2021.120256

Blain, J.A., Ray, D.C. & Wheeley, J.R. 2016. Carbon isotope ($\delta^{13}C_{carb}$) and facies variability at the Wenlock–Ludlow boundary (Silurian) of the Midland Platform, UK. *Canadian Journal of Earth Sciences 53*, 1–6. DOI 10.1139/cjes-2015-0194

Brett, C.E., McLaughlin, P.I., Histon, K., Schindler, E. & Ferretti, A. 2012. Time-specific aspects of facies: state of the art, examples, and possible causes. *Palaeogeography, Palaeoclimatology, Palaeoecology 367–368*, 6–18. DOI 10.1016/j.palaeo.2012.10.009

Calner, M. 2005. Silurian carbonate platforms and extinction events—ecosystem changes exemplified from Gotland, Sweden. *Facies 51(1)*, 584–591. DOI 10.1007/s10347-005-0050-0

Calner, M. 2008. Silurian global events – at the tipping point of climate change, 21–57. *In* Elewa, A.M.T. (ed.) *Mass Extinction*. Springer, Berlin & Heidelberg. DOI 10.1007/978-3-540-75916-4_4

Calner, M. & Säll, E. 1999. Transgressive oolites onlapping a Silurian rocky shoreline unconformity, Gotland, Sweden. *GFF 121(2)*, 91–100. DOI 10.1080/11035899901212091

Calner, M., Lehnert, O. & Nõlvak, J. 2010. Palaeokarst evidence for widespread regression and subaerial exposure in the middle Katian (Upper Ordovician) of Baltoscandia: Significance for global climate. *Palaeogeography, Palaeoclimatology, Palaeoecology 296(3)*, 235–247. DOI 10.1016/j.palaeo.2009.11.028

Calner, M., Lehnert, O. & Jeppsson, L. 2012. New chemostratigraphic data through the Mulde Event interval (Silurian, Wenlock), Gotland, Sweden. *GFF 134(1)*, 65–67. DOI 10.1080/11035897.2012.670015

Cocks, L.R.M., Holland, C.H. & Richards, R.B. 1992. Revised Correlation of Silurian Rocks in the British Isles. *The Geological Society London, Special Report 21*, 1–32. DOI 10.1144/SR21

Coe, A.L. & Ray, D.C. 2022. Chapter 8. Sequence stratigraphy: using changes in relative sea-level and sediment supply to divide, correlate and understand the stratigraphical record, 141–160. *In* Coe, A.L. (ed.) *Deciphering Earth's History: The Practice of Stratigraphy*. Geological Society London, GSL Geoscience in Practice. *https://www.geolsoc.org.uk/GIP001* DOI 10.1144/GIP1-2022-44

Corfield, R.M., Siveter, D.J., Cartlidge, J.E. & McKerrow, W.S. 1992. Carbon isotope excursion near the Wenlock-Ludlow, (Silurian) boundary in the Anglo-Welsh area. *Geology 20(4)*, 371–374. DOI 10.1130/0091-7613(1992)020<0371:CIENTW>2.3.CO;2

Cotter, E. & Link, J.E. 1993. Deposition and diagenesis of Clinton ironstones (Silurian) in the Appalachian Foreland Basin of Pennsylvania. *GSA Bulletin 105(7)*, 911–922. DOI 10.1130/0016-7606(1993)105<0911:DADOCI>2.3.CO;2

Cramer, B.D. & Jarvis, I. 2020. Chapter 11: Carbon isotope stratigraphy, 309–343. *In* Gradstein, F.M., Ogg, J.G., Schmitz, M.D. & Ogg, G.M. (eds) *Geologic Time Scale 2020, Volume 1*. Elsevier, Amsterdam. DOI 10.1016/B978-0-12-824360-2.00011-5

Cramer, B.D., Kleffner, M.A. & Saltzman, M.R. 2006. The Late Wenlock Mulde positive carbon isotope ($\delta^{13}C_{carb}$) excursion in North America. *GFF 128(2)*, 85–90. DOI 10.1080/11035890601282085

Cramer, B.D., Brett, C.E., Melchin, M.J., Männik, P., Kleffner, M.A., McLaughlin, P.I., Loydell, D.K., Munnecke, A., Jeppsson, L., Corradini, C., Brunton, F.R. & Saltzman, M.R. 2011. Revised correlation of Silurian provincial series of North America with global and regional chronostratigraphic units and $\delta^{13}C_{carb}$ chemostratigraphy. *Lethaia 44(2)*, 185–202. DOI 10.1111/j.1502-3931.2010.00234.x

Cramer, B.D., Condon, D.J., Söderlund, U., Marshall, C., Worton, G.J., Thomas, A.T., Calner, M., Ray, D.C., Perrier, V., Boomer, I., Patchett, P.J. & Jeppsson, L. 2012. U-Pb (zircon) age constraints on the timing and duration of Wenlock

(Silurian) paleocommunity collapse and recovery during the "Big Crisis". *GSA Bulletin 124(11–12)*, 1841–1857. DOI 10.1130/B30642.1

Danielsen, E.M., Cramer, B.D. & Kleffner, M.A. 2019. Identification of a global sequence boundary within the upper Homerian (Silurian) Mulde Event: High-resolution chronostratigraphic correlation of the midcontinent United States with Sweden and the United Kingdom. *Geosphere 15(3)*, 839–855. DOI 10.1130/GES01685.1

Fry, C.R., Ray, D.C., Wheeley, J.R., Boomer, I., Jarochowska, E. & Loydell, D.K. 2017. The Homerian carbon isotope excursion (Silurian) within graptolitic successions on the Midland Platform (Avalonia), UK: implications for regional and global comparisons and correlations. *GFF 139(4)*, 301–313. DOI 10.1080/11035897.2017.1388280

Frýda, J. & Frýdová, B. 2014. First evidence for the Homerian (late Wenlock, Silurian) positive carbon isotope excursion from peri-Gondwana: new data from the Barrandian (Perunica). *Bulletin of Geosciences 89(3)*, 617–634. DOI 10.3140/bull.geosci.1493

Gardiner, C.I. 1920. The Silurian rocks of May Hill, with an appendix on two trilobites by F.R. Cowper Reed. *Proceedings of the Cotteswold Naturalists' Field Club 20(3)*, 185–222.

Golonka, J., Porębski, S.J. & Waśkowska, A. 2023. Silurian paleogeography in the framework of global plate tectonics. *Palaeogeography, Palaeoclimatology, Palaeoecology 622*, 111597. DOI 10.1016/j.palaeo.2023.111597

Hillier, R.D., Waters, R.A., Davies, J.R., Higgs, K.T. & Molyneux, S.G. 2023. Late Silurian event stratigraphy and facies of South Wales and the Welsh Borderland, United Kingdom. *Geological Magazine 160(11)*, 2010–2055. DOI 10.1017/S0016756824000086

Holland, C.H. & Lawson, J.D. 1963. Facies patterns in the Ludlovian of Wales and the Welsh Borderland. *Geological Journal 3(2)*, 269–288. DOI 10.1002/gj.3350030205

Hughes, H.E. & Ray, D.C. 2016. The carbon isotope and sequence stratigraphic record of the Sheinwoodian and lower Homerian stages (Silurian) of the Midland Platform, UK. *Palaeogeography, Palaeoclimatology, Palaeoecology 445*, 97–114. DOI 10.1016/j.palaeo.2015.12.022

Hurst, J.M., Hancock, N.J. & McKerrow, W.S. 1978. Wenlock stratigraphy and palaeogeography of Wales and the Welsh Borderland. *Proceedings of the Geologists' Association 89(3)*, 197–226. DOI 10.1016/S0016-7878(78)80012-1

Jenkyns, H. 1995. Carbon-isotope stratigraphy and paleoceanographic significance of the Lower Cretaceous shallow-water carbonates of Resolution Guyot, Mid-Pacific Mountains, 99–104. In Winterer, E.L., Sager, W.W., Firth, J.V. & Sinton, J.M. (eds) Proceedings of the Ocean Drilling Program 143, Scientific Results. DOI 10.2973/odp.proc.sr.143.213.1995

Johnson, M.E. 2006. Relationship of Silurian sea-level fluctuations to oceanic episodes and events. *GFF 128(2)*, 115–121. DOI 10.1080/11035890601282115

Kaljo, D. & Martma, T. 2006. Application of carbon isotope stratigraphy to dating the Baltic Silurian rocks. *GFF 128(2)*, 123–129. DOI 10.1080/11035890601282123

Lawson, J.D. 1954. The Silurian Succession at Gorsley (Herefordshire). *Geological Magazine 91(3)*, 227–237. DOI 10.1017/S0016756800065183

Lawson, J.D. 1955. The Geology of the May Hill Inlier. *Quarterly Journal of the Geological Society of London 111(1–4)*, 85–116. DOI 10.1144/GSL.JGS.1955.111.01-04.06

Loydell, D.K. 1998. Early Silurian sea-level changes. *Geological Magazine 135(4)*, 447–471. DOI 10.1017/S0016756898008917

Loydell, D.K. 2007. Early Silurian positive $\delta^{13}C$ excursions and their relationship to glaciations, sea-level changes and extinction events. *Geological Journal 42(5)*, 531–546. DOI 10.1002/gj.1090

Manda, Š., Štorch, P., Frýda, J., Slavík, L. & Tasáryová, Z. 2019. The mid-Homerian (Silurian) biotic crisis in offshore settings of the Prague Synform, Czech Republic: Integration of the graptolite fossil record with conodonts, shelly fauna and carbon isotope data. *Palaeogeography, Palaeoclimatology, Palaeoecology 528*, 14–34. DOI 10.1016/j.palaeo.2019.04.026

Marshall, C., Thomas, A.T., Boomer, I. & Ray, D.C. 2012. High resolution $\delta^{13}C$ stratigraphy of the Homerian (Wenlock) of the English Midlands and Wenlock Edge. *Bulletin of Geosciences 87(4)*, 669–679. DOI 10.3140/bull.geosci.1306

McAdams, N.E.B., Cramer, B.D., Bancroft, A.M., Melchin, M.J., Devera, J.A. & Day, J.E. 2018. Integrated $\delta^{13}C_{carb}$, conodont, and graptolite biochemostratigraphy of the Silurian from the Illinois Basin and stratigraphic revision of the Bainbridge Group. *GSA Bulletin 131(1–2)*, 335–352. DOI 10.1130/B32033.1

McLaughlin, P.I., Emsbo, P. & Brett, C.E. 2012. Beyond black shales: The sedimentary and stable isotope records of oceanic anoxic events in a dominantly oxic basin (Silurian; Appalachian Basin, USA). *Palaeogeography, Palaeoclimatology, Palaeoecology 367–368*, 153–177. DOI 10.1016/j.palaeo.2012.10.002

Melchin, M.J., Sadler, P.M. & Cramer, B.D. 2020. Chapter 21: The Silurian Period, 695–732. *In* Gradstein, F.M., Ogg, J.G., Schmitz, M.D. & Ogg, G.M. (eds) *Geologic Time Scale 2020, Volume 2*. Elsevier, Amsterdam. DOI 10.1016/B978-0-12-824360-2.00021-8

Pässler, J.-F., Jarochowska, E., Ray, D.C., Munnecke, A. & Worton, G. 2014. Aphanitic buildup from the onset of the Mulde Event (Homerian, middle Silurian) at Whitman's Hill, Herefordshire, UK: ultrastructural insights into proposed microbial fabrics. *Estonian Journal of Earth Sciences 63(4)*, 287–292. DOI 10.3176/earth.2014.32

Phipps, C.B. & Reeve, F.A.E. 1967. Stratigraphy and geological history of the Malvern, Abberley and Ledbury Hills. *Geological Journal 5(2)*, 339–368. DOI 10.1002/gj.3350050209

Porębska, E., Kozłowska-Dawidziuk, A. & Masiak, M. 2004. The *lundgreni* event in the Silurian of the East European Platform, Poland. *Palaeogeography, Palaeoclimatology, Palaeoecology 213(3)*, 271–294. DOI 10.1016/j.palaeo.2004.07.013

Ratcliffe, K.T. 1991. Palaeoecology, taphonomy and distribution of brachiopod assemblages from the Much Wenlock Limestone Formation of England and Wales. *Palaeogeography, Palaeoclimatology, Palaeoecology 83(4)*, 265–293. DOI 10.1016/0031-0182(91)90056-W

Ratcliffe, K.T. & Thomas, A.T. 1999. Carbonate depositional environments in the late Wenlock of England and Wales. *Geological Magazine 136(2)*, 189–204. DOI 10.1017/S0016756899002538

Ray, D.C. & Butcher, A. 2010. Sequence stratigraphy of the type Wenlock area (Silurian), England. *Bollettino della Società Paleontologica Italiana 49(1)*, 47–54.

Ray, D.C., Brett, C.E., Thomas, A.T. & Collings, A.V.J. 2010. Late Wenlock sequence stratigraphy in central England. *Geological Magazine 147(1)*, 123–144. DOI 10.1017/S0016756809990197

Ray, D.C., Collings, A.V.J., Worton, G.J. & Jones, G. 2011. Upper Wenlock bentonites from Wren's Nest Hill, Dudley: comparisons with prominent bentonites along Wenlock Edge, Shropshire, England. *Geological Magazine 148(4)*, 670–681. DOI 10.1017/S0016756811000288

Ray, D.C., Richards, T.D., Brett, C.E., Morton, A. & Brown, A.M. 2013. Late Wenlock sequence and bentonite stratigraphy in the Malvern, Suckley and Abberley Hills, England. *Palaeogeography, Palaeoclimatology, Palaeoecology 389*, 115–127. DOI 10.1016/j.palaeo.2013.03.024

Ray, D.C., Jarochowska, E., Röstel, P., Worton, G., Munnecke, A., Wheeley, J.R. & Boomer, I. 2020. High-resolution correlation of the Homerian carbon isotope excursion (Silurian) across the interior of the Midland Platform (Avalonia), UK. *Geological Magazine 157(4)*, 603–620. DOI 10.1017/S0016756819001146

Samtleben, C., Munnecke, A. & Bickert, T. 2000. Development of facies and C/O-isotopes in transects through the Ludlow of Gotland: Evidence for global and local influences on a shallow-marine environment. *Facies 43(1)*, 1–38. DOI 10.1007/BF02536983

Squirrell, H.C. & Tucker, E.V. 1960. The geology of the Woolhope Inlier (Herefordshire). *Quarterly Journal of the Geological Society 116(1–4)*, 139–181. DOI 10.1144/gsjgs.116.1.0139

Torsvik, T.H., Trench, A., Svensson, I. & Walderhaug, H.J. 1993. Palaeogeographic significance of mid-Silurian palaeomagnetic results from southern Britain-major revision of the apparent polar wander path for eastern Avalonia. *Geophysical Journal International 113(3)*, 651–668. DOI 10.1111/j.1365-246X.1993.tb04658.x

Trotter, J.A., Williams, I.S., Barnes, C.R., Männik, P. & Simpson, A. 2016. New conodont $\delta^{18}O$ records of Silurian climate change: Implications for environmental and biological events. *Palaeogeography, Palaeoclimatology, Palaeoecology 443*, 34–48. DOI 10.1016/j.palaeo.2015.11.011

Ziegler, A.M., Rickards, R.B., McKerrow, W.S. & Boucot, A.J. 1974. Correlation of the Silurian Rocks of the British Isles, 1–154. *In* Berry, W.B.N. & Boucot, A.J. (eds) *Geological Society of America Special Paper.* DOI 10.1130/SPE154-p1